Environmental Science Nano

ROYAL SOCIETY OF CHEMISTRY

PAPER

View Article Online
View Journal | View Issue

Cite this: *Environ. Sci.: Nano*, 2023, **10**, 1413

Polycarbonate nanoplastics and the *in vitro* assessment of their toxicological impact on liver functionality†

Valentina Tolardo,‡[ab] Alessio Romaldini, ‡[c] Francesco Fumagalli,[d] Andrea Armirotti,[e] Marina Veronesi, [fg] Davide Magrì, §[d] Stefania Sabella,*[c] Athanassia Athanassiou [a] and Despina Fragouli *[a]

Herein, we demonstrate the formation of polycarbonate (PC) nanoplastics (NPs) through laser ablation of solid PC films in water. We prove that the size of the produced particles depends directly on the laser energy fluence, ranging between a few tens and a few hundreds of nanometers. Focusing on NPs of the smallest size range, the chemical characterization proves that they are composed of PC, while their surface is highly oxidized, similar to the PC fragments derived from natural photo-degradation processes. Together with the PC-NPs, additional photo-degradation by-products are formed, similar to the ones expected from environmentally exposed plastics. With the aim of providing reliable insights into the potentially detrimental effects of PC-based plastic litter on human health, upcyte® human hepatocytes were selected as a hepatic cellular model for assessing the hepatotoxicity of PC-NPs. Although no cytotoxic effects were observed at low concentrations (up to 40 μg mL^{-1}), an alteration of the cytochrome P450 system (CYP3A4, CYP2C9, and CYP1A2) and a reduction of the albumin production were found. Interestingly, we prove that these cytotoxic effects can be attributed to both the nano-particulate matter (*i.e.*, the NPs) and the molecular matter (*i.e.*, the photo-degradation by-products). Although far from the recapitulation of the real fate of NPs in the environment, with this novel approach we demonstrate the possibility of obtaining in a single step an environmentally pertinent composition of PC photo-degradation products, applied on a physiologically meaningful hepatic cellular model for human exposure studies.

Received 20th October 2022,
Accepted 11th March 2023

DOI: 10.1039/d2en00963c

rsc.li/es-nano

Environmental significance

The biological fate of nanoplastics is mainly evaluated using chemically synthesized nanospheres, not always representative of the environmentally pertinent plastic degradation products including nanofragments and molecular by-products. Their effects on the liver are assessed by short-term toxicological evaluation using standard cell models with a poorly differentiated phenotype and low gene expression of xenobiotic-metabolizing enzymes. Through the single-step formation of polycarbonate photo-degradation mixtures of nanoplastics and molecular by-products, we explore their effects on a realistic human hepatic model, studying within the same experiment the cytotoxicity and the hepatocyte-specific function alterations. As proved, both the particulate matter and the molecular by-products induce specific hepatotoxicity effects. This highlights the necessity to improve the understanding of the potential hazard induced by nanoplastics, through the utilization of relevant human cell models and of more realistic plastic samples, to provide reliable insights into the potentially detrimental effects of plastic litter on human health.

[a] *Smart Materials, Istituto Italiano di Tecnologia, Via Morego, 30, 16163 Genova, Italy. E-mail: despina.fragouli@iit.it*
[b] *Department of Informatics, Bioengineering, Robotics and Systems Engineering, University of Genova, Via All'Opera Pia, 13, 16145 Genova, Italy*
[c] *Nanoregulatory Group, D3 PharmaChemistry, Istituto Italiano di Tecnologia, Via Morego, 30, 16163 Genova, Italy. E-mail: stefania.sabella@iit.it*
[d] *European Commission, Joint Research Centre (JRC), Ispra, Italy*
[e] *Analytical Chemistry Laboratory, Istituto Italiano di Tecnologia, Via Morego, 30, 16163 Genova, Italy*
[f] *D3 PharmaChemistry, Istituto Italiano di Tecnologia, Via Morego, 30, 16163 Genova, Italy*
[g] *Structural Biophysics and Translational Pharmacology, Istituto Italiano di Tecnologia, Via Morego, 30, 16163 Genova, Italy*

† Electronic supplementary information (ESI) available. See DOI: https://doi.org/10.1039/d2en00963c

‡ These authors contributed equally.

§ Current address: GenScript Biotech, B.V. Treubstraat 1, 2288EG, Rijswijk, Netherlands.

Introduction

Plastics, predominantly derived from petrochemicals and, in a lower portion, from renewable sources, show unique properties that make them fundamental components of our everyday life.[1] Not surprisingly, this "plastic addiction" is reflected in our planet's geological history with the term Plasticene (age of plastics) which describes the current chronological period starting from the mid-20th century.[2] From 1950 to 2017, it is estimated that 9.2 billion tons of plastics were produced, and approximately 5.3 billion tons have been discarded, ending up either in landfills or as litter in natural ecosystems.[3] According to a recent study,[4] and assuming that the plastic production and waste generation and management continue at the current pace, the predicted amount of plastics entering the ocean will increase 2.6-fold until 2040. Through photo-degradation, mechanical abrasion and weathering processes, plastic litter breaks into smaller pieces until it reaches the micro- and nano-size scale,[5] generating micro- and nano-plastics (MPs and NPs, respectively). Accumulation and persistence of such small plastic pieces, also directly released by primary sources such as personal care products or textiles, have been found in diverse aquatic organisms as well as in arctic ice,[6,7] sea-salt, drinking water and beer,[8] among others, and also in human feces[9,10] and blood[11] proving that humans are seriously exposed to such types of pollutants.

Nevertheless, the fate and persistence of MPs and NPs in water systems have not been adequately defined. Especially for NPs, little information is available regarding their presence in the environment, and therefore, regarding their effects on living organisms, due to the inadequacy of current analytical methods to study them directly in natural environments[12] and to detect and recover sufficient quantities for further *ex situ* studies.[13,14] Therefore, to explore their interactions with biological systems, commercially available nanoparticles, chemically synthesized and mostly limited to polystyrene (PS) nano-beads,[15–17] are used. Such studies have proved that NPs may penetrate biological membranes affecting many cellular functions.[18] However, several other typologies of plastics are found in the environment such as polyethylene (PE), polypropylene (PP), polyethylene terephthalate (PET), polyvinyl chloride (PVC), and PC[19] among others, and, therefore, the question of how biological systems respond to the different types of NPs is logically raised.

For most of the above studies on NPs, poor information is available on the presence of photo-degradation by-products, naturally occurring during the NP formation, and on the effects that such combination may cause.[20] In fact, it is noted that bisphenol A (BPA), used for the production of PC, and phthalates, which are chemical additives broadly used in plastics, can be released during the degradation process of plastics exposed to the environment,[21] and it has been proved that such substances significantly affect the cell functionalities.[20,22] Therefore, it is a plausible hypothesis that both NPs and by-products of the plastic degradation affect living organisms. To deal with these issues and bridge the gap between the wide variety of NPs naturally produced in the environment through degradation processes and the limited availability of commercial NPs pure from other organic compounds, the exploration of new synthetic approaches for the production of realistic NP dispersions from different source materials is crucial. In this way, reliable toxicological profiles for human health can be obtained.

Plastic particles can enter the body through one of the major routes (dermal absorption, inhalation, or ingestion)[23–25] and arrive *via* the bloodstream to secondary organs, such as the liver. The liver has a central role in detoxifying the body from xenobiotics/toxicants and, thus, the accumulation of MPs or NPs in this organ is a plausible assumption. In fact, it has been proved that PS particles (size range 50 nm–20 μm) accumulate in the liver of mice[26] and Sprague Dawley rats[27] upon exposure by oral gavage. Other *in vivo* studies have also proved that NPs from different source materials accumulate in the liver of fishes.[28,29]

To assess the potential hepatotoxicity of MPs or NPs, *in vitro* studies have been performed mainly using hepatocarcinoma cell lines (such as HepG2 and HepaRG cells) as human hepatic cell models.[30–34] Overall, the data indicate that, at doses in the range of 0–100 μg mL^{-1}, plastic particles induce cell viability reduction, oxidative stress, inflammation, or the formation of binucleated cells (possibly indicative of impaired cytokinesis). However, poor information is currently available on the effects exerted by NPs on hepatocyte-specific functions (*e.g.*, CYP metabolic activity) due to the unsuitability of the HepG2 cells.[35,36] Other cell models, including HepaRG cells and primary human hepatocytes (PHHs), can address such a gap even though, to the best of our knowledge, no studies are currently available for NPs. Moreover, still poor information is available regarding the role of both NPs and their degradation by-products in hepatoxicity and/or in the alteration of the liver functionality, although it has been recently proved that the photo-degradation mixtures of PS fragments induce apoptosis, ROS generation, lysosomal membrane damage, and mitochondrial depolarization in the liver samples of juvenile groupers (*Epinephelus moara*).[20] Furthermore, as reported, BPA (a degradation by-product of PC[21]) has inhibitory effects on the metabolic activity of CYP2C8 and CYP2C19 expressed in microsomes,[37] and determines the alteration of many signalling pathways, modulating the gene expression of downstream CYPs in human hepatocytes.[22] Overall, the presented state-of-the-art analysis evidences that to have a clearer understanding of the plastic impact on human health, both realistic samples of NPs and advanced liver cell models (also accounting for the liver functionality) are needed.

Within this context, in this study, we present a synthetic approach for the controlled production of a realistic mixture of photo-degradation products of PC through laser ablation. After the in-depth characterization of the obtained NPs and

degradation by-products, we assess the biological impact of such a mixture on the human liver using second-generation upcyte® human hepatocytes (UHHs), which are genetically engineered hepatocytes derived from PHHs.[38] Compared to other cell lines, UHHs present many advantages, as they are differentiated hepatocytes isolated from different donors which retain numerous key functionalities exhibited by PHHs, including good catalytic activity of phase-I and -II enzymes,[35,39] epithelial polarization,[38] and sustained synthesis of albumin, urea, lipid, and glycogen.[35,38] We prove that the nature of the final ablation product is similar to the one expected to be derived from the natural photo-degradation of PC macro-fragments.[40–42] In particular, NPs with an oxidized surface and a mean diameter of approximately 30 nm are found dispersed in a liquid containing molecular fragments coming from the PC polymer chain and other components released during the degradation of the plastic. For the hepatotoxicity evaluation, UHHs were preliminarily treated with a wide range of PC-NP concentrations (20–100 μg mL^{-1}) to determine a dose–response curve. After that, concentrations lower than 40 μg mL^{-1} (corresponding to sub-lethal doses) were selected for downstream investigations, finding an alteration of the cytochrome P450 system and the reduction of albumin production. This is attributed to the interactions of both of the components of the PC-NP dispersion with the cells, as revealed by testing the nano-particulate or molecular components separately. Therefore, it can be concluded that the photo-degradation products of PC may affect hepatic functionality. To the best of our knowledge, this is the first study aimed at disclosing *in vitro* the impact of polycarbonate-derived nanopollutants on the human liver through an extended analysis at different levels (gene expression, protein synthesis, and metabolic activity) of key hepatic markers using a physiologically meaningful cellular model for the human exposure (*e.g.*, liver) and a realistic sample of NPs including photo-degradation by-products.

Materials and methods

Fabrication of PC particles

The fabrication of the PC particles was performed by laser ablation of commercial BPA-PC films (Goodfellow Cambridge Ltd., Hamburg, DE). The films, previously purified by ethanol and Milli-Q® water, were immersed in 8 ml of Milli-Q® water and exposed to laser irradiation using a KrF excimer laser (wavelength: 248 nm, pulse duration: 20 ns, repetition rate: 10 Hz, number of pulses: 50, Coherent-CompexPro 110, Utrecht, NL). The laser was coupled with a micromachining apparatus (Optec-MicroMaster, Frameries, BE) in order to irradiate an array on a 4 cm^2 area in an automated way. To investigate the effect of the laser fluence on the ablation product, three different irradiation fluences were used (2.8 J cm^{-2}, 2.1 J cm^{-2}, 0.9 J cm^{-2}). The evaluation of the amount of the PC particles produced in terms of mg mL^{-1} was performed as described in the ESI† section S1.

To obtain dispersions with particles in the nanometric range (PC-NPs), the ablation product after laser irradiation with a fluence of 2.8 J cm^{-2} was filtered (cellulose acetate filters, cut-off 0.22 μm, Millipore) in order to remove the bigger polymer fragments possibly present in the mixture, and the filtrate was concentrated by rotary evaporation treatment at 45 °C (Rotavap System R-100, Buchi Italia S.R.L). In this way NP dispersions with defined concentrations (300 μg mL^{-1}) were obtained.

For the toxicological assessment, the potential presence of bacterial endotoxins was evaluated in each PC-NP dispersion batch using a Pierce™ LAL chromogenic endotoxin quantitation kit (Thermo Scientific™-Thermo Fisher Scientific, Waltham, MA, USA). All batches exhibited an endotoxin concentration lower than 0.5 EU mL^{-1}, which is the limit for medical devices indicated by the US Food and Drug Administration guidelines.[43]

Physicochemical characterization

The hydrodynamic diameter (D_H) and the surface charge of the PC-NPs were determined *via* dynamic light scattering (DLS) and zeta potential (Z-pot) analysis, respectively, using a Zetasizer Nano-ZS (Malvern Instruments, Cambridge, UK) spectrometer at 25 °C. To study the surface charge variation at different pH values, an aliquot of 10 μl of the PC-NP dispersion (300 μg mL^{-1}) was introduced in 1 mL of the following buffer solutions: tris(hydroxymethyl)aminomethane hydrochloride salt (Trizma hydrochloride) in Milli-Q® water (pH 9–8, 0.002 M), phosphate buffer saline in Milli-Q® water (pH 7–6, 0.002 M) and diluted acetic acid in Milli-Q® water with sodium hydroxide (pH 5–4, 0.002 M). All chemicals were purchased from Sigma-Aldrich, Milano, IT.

The colloidal stability of the PC-NPs in complete HHPM (*i.e.*, fully supplemented hepatocyte high performance medium; upcyte Technologies GmbH, Hamburg, DE) and their surface charge were evaluated as described in the ESI† section S2.

The morphology of the PC-NPs was explored using a transmission electron microscope (TEM) (JEM-101, JEOL, Tokyo, Japan) equipped with a thermionic source (W filament) and with an accelerating voltage of 100 kV. The PC particle dispersions were drop cast on ultrathin carbon layered Cu grids (CF300-CU-UL) (Electron Microscopy Science, Hatfield, Pennsylvania) at room temperature (RT). The size distribution of the particles was determined using ImageJ and Origin Pro 2018 v9.5 software.

Chemical characterization was performed with Raman analysis (LabRam HR800, Horiba Jobin-Yvon Inc., France) and the surface chemistry was evaluated by X-ray photoelectron spectroscopy (XPS) using an Axis Ultra spectrometer (Kratos Analytical) with an Al Kα source ($h\nu$ = 1486.6 eV) operated at 15 kV with an emission current of 10 mA and an X-ray spot size of 100 × 100 μm^2. Details on the experimental processes are provided in the ESI† section S3.

Separation of PC-NPs from the dispersant

To separate the two main components of the PC-NP dispersion, Amicon® Ultra 0.5 mL centrifugal filters (Sigma Aldrich-Merck KGaA, Darmstadt, DE) were used following the manufacturer's instructions. A 3 kDa cutoff was selected. Briefly, the PC-NP dispersion (629 μg mL^{-1}) was centrifuged at 14 000*g* for 30 minutes at RT. The corresponding ultrafiltrate, called "dispersant", was collected. The concentrated sample, called "isolated PC-NPs", was recovered by a reverse spin step at 1000*g* for 2 minutes at RT (final concentration equal to 1533 μg mL^{-1}). In parallel, Milli-Q® water was ultrafiltered, obtaining the "filtered water", used as a negative control.

For the cell treatment, the dispersant was supplemented to the complete HHPM by adding a volume equal to the volume of the PC-NP dispersion used for preparing a stimulation medium at 40 μg mL^{-1}. The filtered water was added considering the same volume of the dispersant. The isolated PC-NPs were dispersed down to 40 μg mL^{-1} in complete HHPM. In all the stimulation media, along with the un-supplemented control medium, Milli-Q® water was added in order to obtain the same aqueous fraction (about 6.4%).

^{1}H nuclear magnetic resonance and liquid chromatography-mass spectrometry (LC-MS) analysis

The molecular components of the dispersant were explored by NMR and high-resolution mass spectrometry, without any further purification as described in the ESI† sections S4 and S5.

Cell culture

Second-generation UHHs (derived from the donor 653–03; upcyte® Technologies GmbH, Hamburg, DE) were cultured as previously reported by Romaldini *et al.*[44] After thawing, cells were expanded for 2 passages in collagen-coated tissue culture flasks (VWR, Radnor, PA, USA) and, at passage 3 (P3), were treated with the PC-NP dispersions in collagen-coated flat bottom 24- or 96-well plates (Corning Incorporated, Corning, NY, USA) as described below. At P3, the number of viable cells was higher than 92.9%, as revealed by the trypan blue (Sigma Aldrich-Merck KGaA, Darmstadt, DE) exclusion test. For avoiding alterations of cytochrome P450 activity, antibiotics were not used at any passage.

Cell viability assay

The resazurin reduction test was used for determining the cell viability after treatment with PC-NP dispersions as described in the ESI† section S6.

Cytotoxicity assay

The CytoTox96® non-radioactive cytotoxicity assay (Promega Corporation, Madison, WI, USA) was used for evaluating the cell membrane integrity after the treatment with PC-NP dispersions as described in the ESI† section S7.

Reverse transcription and quantitative real-time PCR

At P3, UHHs were seeded into collagen-coated flat bottom 24-well plates (growth area: ~2.0 cm^2; ~9.5 × 10^4 cells per cm^2) and, at the confluence, were treated with increasing concentrations of the PC-NP dispersions (0.667 mL/24-well) for 24 or 48 hours. Using the same experimental setting, confluent cells were also treated with the isolated PC-NPs, the dispersant, or the filtered water, as described above. Detailed description of the experimental process is presented in the ESI† section S8.

Western blot

In parallel with gene expression analysis, protein content analysis was performed *via* western blot as described in the ESI† section S9.

CYP2C9 activity assay

The metabolic conversion of 7-methoxy-4-trifluoromethylcoumarin (MFC; Sigma Aldrich-Merck KGaA, Darmstadt, DE) to 7-hydroxy-4-trifluoromethylcoumarin (HFC) by CYP2C9 was evaluated as described in the ESI† section S10.

Statistical analysis

Statistical analysis was run on Prism (GraphPad Software, San Diego, CA, USA). Differences were considered statistically significant as the *p*-value was lower than 0.0500 (further information in the ESI† section S11).

Results and discussion

Laser ablation has been proved a valuable top-down method to produce a realistic model of PET-NPs found in aquatic systems.[42,45] To further explore its usability for other types of

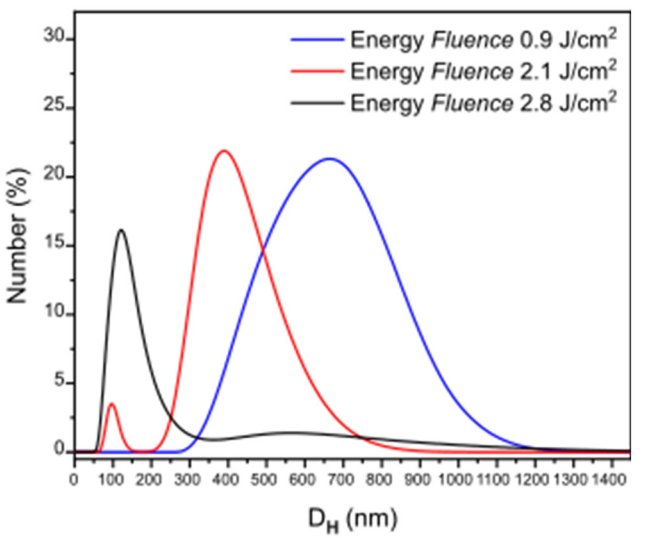

Fig. 1 Hydrodynamic diameter (D_H) distribution of particles formed at three different energy fluences.

polymers and its versatility to produce different particle sizes, PC films were used as targets for the laser ablation process, and the ablation products after irradiation with different laser fluences (F) were analyzed. During ablation, photons of specific energy per unit area interact with the PC polymer substrate, inducing the fragmentation of the polymer into smaller pieces which are ejected and dispersed in the liquid environment.[46] As shown in the DLS spectra of Fig. 1, the variation of the fragments' size is directly related to the F of the system. With increasing F, the number of the photons that arrive to the specific area of the polymer surface increases, causing a more intense fragmentation resulting in smaller pieces. In particular, it can be seen that almost all the particles produced at the highest F (2.8 J cm^{-2}) have a D_H in the nanometer range, lower than 200 nm. Working at an F of 2.1 J cm^{-2} two populations are produced, one in the submicron range with sizes peaking at around 400 nm, while there is also a small amount of particles in the nanosize range (peak at D_H *ca.* 90 nm). Smaller irradiation F (0.9 J cm^{-2}) results in the formation of particles with highly polydisperse sizes in the submicron range, peaking at a D_H of 700 nm.

Focusing on the F that generated the smallest NPs (2.8 J cm^{-2}), the chemical characterization of the ablation product was performed with Raman analysis. As shown in the spectra of Fig. 2, the comparison with the pristine PC film shows no significant difference, with the main characteristic peaks of the PC chemical structure appearing in both cases,[47–49] indicating that the laser ablation process in water does not affect significantly the chemical composition of the polymer. Specifically, in both spectra are present a peak at 896 cm^{-1} associated with O–C(O)–O stretching, a set of three bands, 1118 cm^{-1}, 1186 cm^{-1} and 1245 cm^{-1} attributed to the C–O–C stretching, and bands which correspond to the phenyl ring vibration and stretching mode (bands between 500 and 700 cm^{-1}, and 825 cm^{-1} for vibration and 1611 cm^{-1} for the stretching mode). The band at 1460 cm^{-1} is attributed to the CH_3 bending vibration and the one at 1787 cm^{-1} to the C═O stretching[47–49] (all peaks are characterized as shown in Table S1, ESI†).

To further study the PC-NPs, the ablation product after irradiation with an F of 2.8 J cm^{-2} was filtered to remove any possible big fragments, and the final material was concentrated to have a stock solution of 300 μg mL^{-1}. The morphology of the PC-NPs was investigated by TEM analysis, as shown in Fig. 3A. Specifically, the PC-NPs have an almost spherical shape, with a mean size of 31.5 nm (scatter intervals = −20.3, +48.9 nm) (size distribution analysis: Fig. S1, ESI†), confirming the fact that with the specific top-down approach, particles in the nanometer size range are formed.

The surface charge of the PC-NPs was determined with the Z-pot study at different pH values. As shown in Fig. 3B, the PC-NPs are negatively charged, showing lower Z-pot absolute values with the reduction of the pH. This behavior indicates that on the surface of the PC-NPs, weak acid groups may be present, such as carboxylic groups, since similar Z-pot variation is typically observed in colloidal systems with such groups present on the surface of the dispersants.[42,50]

The surface chemistry of the PC-NPs was further studied by XPS. By the survey spectra analysis (Fig. S2, ESI†), the O/C elemental ratio is higher in the NPs (O/C_{NPs} = 1.53 ± 0.04) compared to the PC film ($O/C_{pristine}$ = 0.21 ± 0.02), demonstrating the higher presence of the oxygen element on

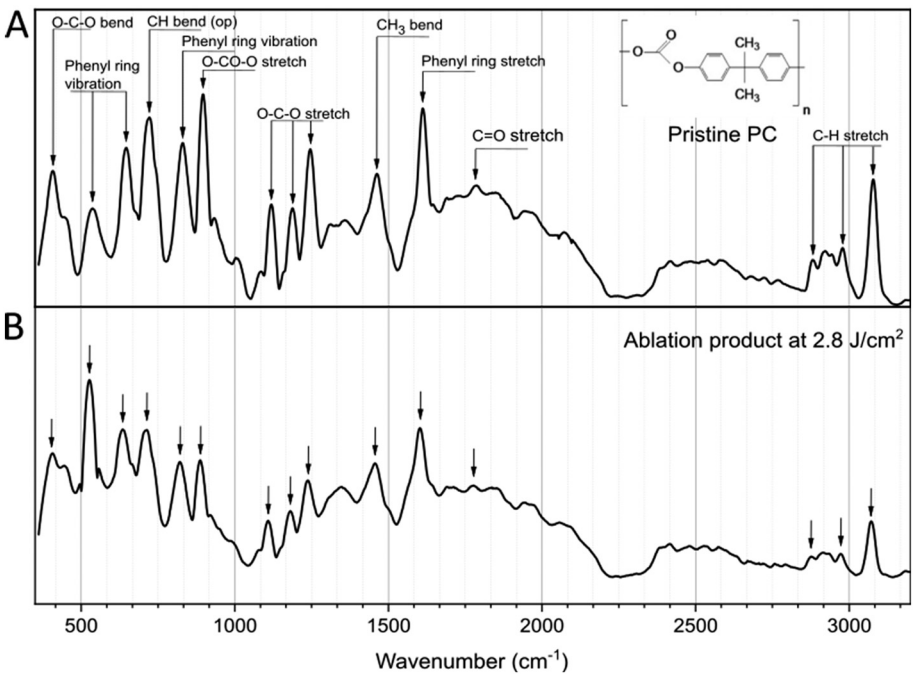

Fig. 2 Raman analysis of pristine PC (A) and the ablation product (B) after irradiation at F = 2.8 J cm^{-2}. Inset: Chemical structure of the PC.

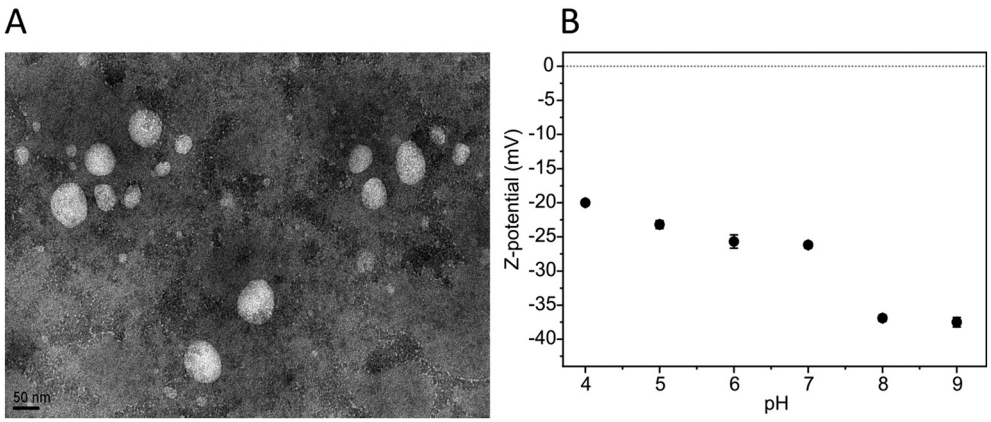

Fig. 3 PC-NP morphology and surface charge. (A) A representative TEM image of PC-NPs (30 000×; scale bar = 50 nm). (B) PC-NP Z-pot measured at different pH values.

the surface of the NPs compared to the bulk films. Relative elemental compositions are presented in Table S2 (ESI†). In addition to the expected presence of the C and O elements (from the sample) and of F from the Teflon substrate, signals from Si, Ca, and Na were also detected. Ca and Na are likely present in the water dispersion and concentrate on the NP surface during the drying step of the XPS analysis preparation, whereas Si (in traces) is often used as a liner in the preparation of several commercial polymers and likely originates from the bulk PC sheets. A more detailed understanding of the NP surface chemical environment can be obtained from the high-resolution spectra analysis of the C1s peak (Fig. 4 and Table S3, ESI†). The deconvolution and analysis of the C1s peak envelope were implemented according to the guidelines of Gengenbach *et al.*[51] The component located at 284.8 eV includes signals from both aromatic and aliphatic C–H/C–C groups, and its contribution decreases in the NP sample (65.3%) compared to the pristine film (83.4%). The peak at 286.3 eV is assigned to the contribution from C–O–C/C–OH groups, and their relative abundance markedly increases in the NPs (19.9%) compared to the pristine polymer (8.7%). A slight decrease is instead observed in the concentration of O═C(–O)$_2$ groups (binding energy: 290.4 eV) of the PC-NPs compared to the film surface (PC NPs: 2.2% and pristine PC: 2.6%). Furthermore, in the PC-NPs a new peak at 287.7 eV representative of the C═O group appears, and the increase of the O═C–O component observed at 288.7 eV is clear (pristine PC: 1.9%, likely originating from adventitious contamination occurring during sample preparation, and PC NPs: 8.9%).[52]

Therefore, the principal exposed groups are groups with oxygen (–COO$^-$, C═O, C–O–C, C–OH) such as diphenyl groups, aromatic esters, aromatic aldehydes, carboxylic acids, and aliphatic esters,[53–56] usually formed on the PC surface upon light exposure.[52] Qualitatively similar surface chemistry was observed on plastic NPs obtained from milling and filtering naturally weathered plastic waste.[57] In particular, these groups typically occur as by-products during

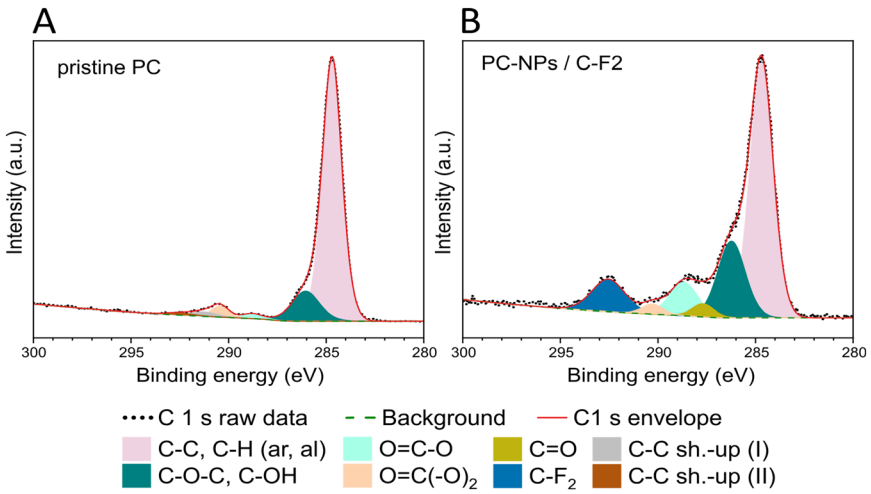

Fig. 4 XPS C1s high resolution spectra of the pristine polymer (A) and of the as-synthesized NPs (B) with the corresponding deconvolutions. NP dispersion drop-cast on the Teflon (C_2F_4) substrate.

photodegradation of PC, with their generation proceeding *via* photo-Fries chemistry driven by UV with wavelengths <300 nm and *via* photo-oxidation at longer wavelengths.[58] In the photo-Fries mechanism, the energy absorbed from UV irradiation promotes the scission of the carbonate linkage, forming two primary free radicals. The free radicals then rearrange to form phenyl salicylates and dihydroxybenzophenones, and other groups such as dihydroxybiphenyl and hydroxydiphenyl ether groups.[53,59] Meanwhile, the photo-oxidation occurs *via* a three stage reaction,[53,59–61] the UV radiation is absorbed by the polymer, causing the hydrogen atom abstraction from the methyl groups, forming free radicals and thus initiating a chain scission reaction which propagates. In the presence of oxygen, the methyl side chains are photo-oxidised into hydroperoxide intermediates, which are transformed into tertiary alcohols and ketones. Therefore, it is possible to conclude that these NPs mimic well the resulting chemical composition of PC nano-objects undergoing outdoor (sunlight induced) weathering in the natural environment. In fact, considering the broad sunlight spectrum it is highly possible that both photo-oxidation and photo-Fries rearrangement reactions take place on the PC under outdoor exposure.[62,63]

It is well known that during the degradation process of PC bulk plastics[64] and MPs[21] exposed to the environment, not only the composition of the solid is modified but also various by-products are released from the polymer structure. To identify the possible molecular by-products formed or released into water during the fabrication process of PC-NPs upon laser ablation, NMR and high-resolution UPLC-MS analysis were performed in the dispersant after the removal of the PC-NPs from the mixture upon filtration. In agreement with a previous study on the identification of the photo-degradation by-products of the PC-MPs,[21] one of the components carries, as a moiety, the structure of BPA (as demonstrated by the NMR analysis and fragment at 227.1080 *m*/*z* observed in the corresponding MS/MS spectrum; Fig. S3 and S4, ESI†) which may leach from the polymer during the ablation process. Apart from the BPA leachate, some BPA by-products are also identified, naturally occurring during the photodegradation process of the PC exposed to the environment, due to the BPA photolysis. Considering the four different transformation mechanisms of BPA during photolysis, such as ring modification, isopropylidene bridge modification, isopropylidene bridge cleavage, and ring cleavage,[65–67] by-products attributed to at least two of them were identified. As shown in Fig. S4,† the presence of the P271 compound in the dispersant indicates the carbonylation and carboxylation in the *ortho*-position of the BPA rings as one of the conspicuous ways of ring modification. The identification of the P243a by-product (Fig. S5, ESI†) also indicates the ring modification by polyhydroxylation due to the attacks of diverse reactive oxygen species (ROS) or electron transfer. Finally, the possible presence of the P243b may also indicate the isopropylidene bridge modification as a photolysis path through the initiation by hydrogen abstraction to cultivate the isopropylidene-BPA radical, which is further modified by ROS or dissolved O_2. Concerning the identification of the P243a and P243b products (Fig. S5, ESI†), it should be mentioned that the lack of available reference MS/MS spectra allows a structure assignment only based on manual interpretation of MS/MS fragmentation. In both spectra, the intact species are clearly detectable (at 243.10 *m*/*z*), while the presence of "twin" ions at 227/228 (bottom spectrum) clearly indicates the presence of the bi-hydroxyphenyl rings in the molecule.

Based on these data, it is possible to conclude that with the laser ablation process a PC-NP mixture is produced with products similar to the ones expected to be formed by the natural photo-degradation process of PC fragments exposed to the environment. Indeed, as already discussed, during the degradation process of the PC plastic litter exposed to the environment, not only NPs but also many other molecular by-products, such as residual unpolymerized monomers, oligomers and other degradation products of the plastic itself are released or formed.[68,69] Therefore, the herein proposed method offers the possibility of mimicking this procedure and obtaining NP dispersions, which also contain other photo-degradation by-products of the pristine plastic. This enables a more realistic exploration of the biological fate of the PC litter exposed to the environment and subjected to degradation.

After confirming that PC-NP dispersions formed *via* laser-ablation can be considered a representative model of the PC photo-degradation products formed in the outdoor environment, the potential toxicological impact of the fabricated material on the human liver was investigated, taking advantage of hepatocyte-specific functions exhibited by UHHs.

The colloidal stability of PC-NPs dispersed in complete HHPM (*i.e.*, the fully supplemented culture medium of UHHs) was assessed by DLS analysis using the experimental time points applied for the cellular experiments (up to 48 hours; Fig. S6A and Table S4, ESI†). Immediately after the dispersion in complete HHPM (0 hours), the size distribution profile of PC-NPs shows two peaks, approximately close to 159 nm (peak #2, relative intensity: 42.7%) and 4500 nm (peak #3, relative intensity: 1.7%). Peak #2 corresponds to the main subset of PC-NPs and refers to sizes comparable to those of PC-NPs dispersed in Milli-Q® water (Fig. S6B, ESI†). Peak #3 indicates the presence of large agglomerates/aggregates, which were absent in Milli-Q® water. The peak found at smaller sizes (peak #1, showing 55.5% of relative intensity) refers likely to the protein components of the medium[70] (Fig. S6C, ESI†). After 24 hours of incubation, while peak #2 shifted towards larger sizes (about 529 nm) suggesting a partial tendency of agglomeration/aggregation, peak #3 tended to disappear (revealed only in 1 out of 3 measurements). At 48 hours, the size distribution profile remained almost unvaried with respect to that at 24 hours, indicating no relevant and/or additional changes in the colloidal stability of the dispersion.

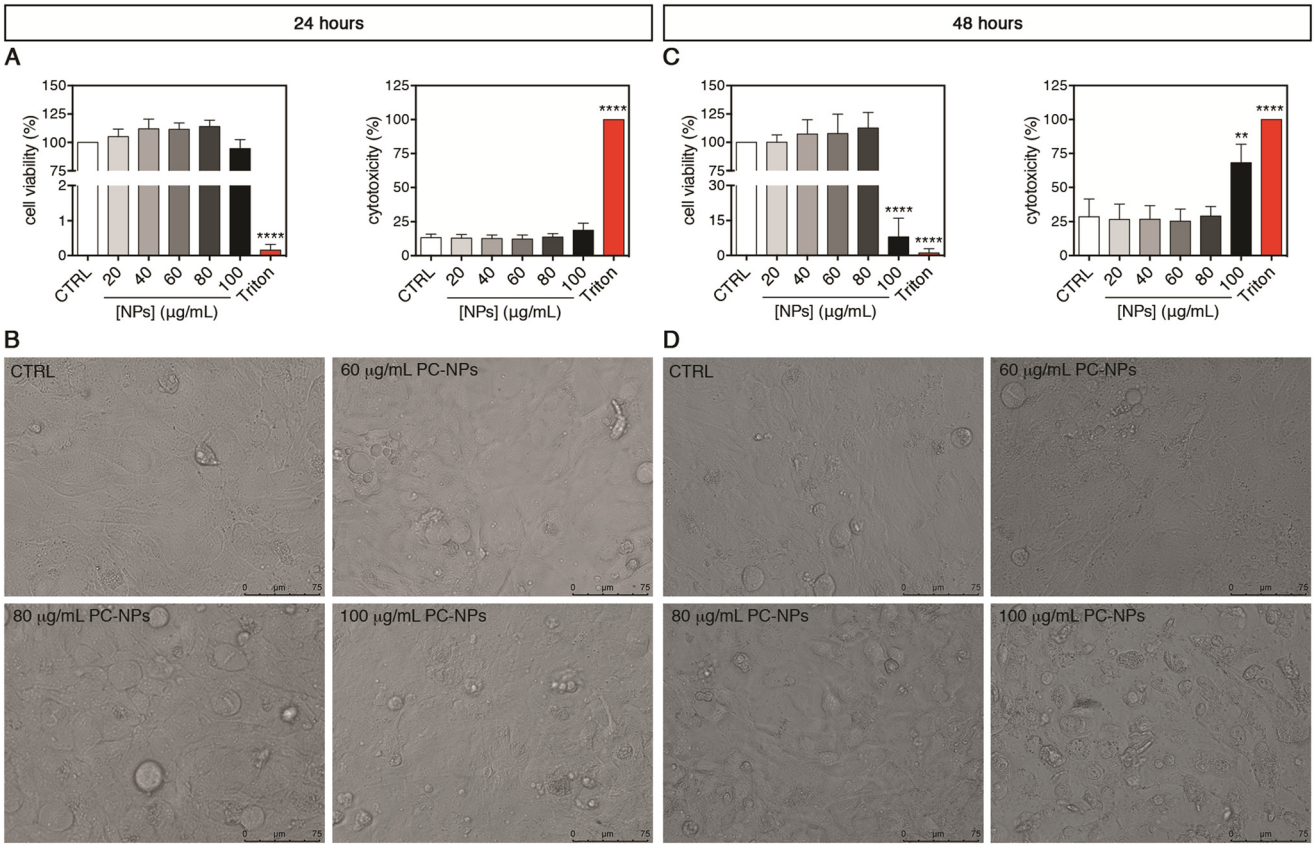

Fig. 5 PC-NP toxic impact on upcyte® hepatocyte 2D cultures. (A and C) Cell viability by resazurin reduction assay (left panel) and cell membrane integrity by cytotoxicity assay (right panel) upon 24 (A) and 48 hours of exposure (C). "CTRL" refers to un-treated control cells and "Triton" to the positive control, represented by cells treated with 0.03% Triton X-100. Results are means ± SD of three independent experiments. The symbols ** and **** refer to $p = 0.0010$ and $p < 0.0001$, respectively, calculated *versus* CTRL (ordinary one-way ANOVA). (B and D) Representative images by optical microscopy relative to cells treated with different PC-NP concentrations or un-treated for 24 (B) or 48 hours (D). All the images are 40× magnifications (scale bar = 75 μm).

The Z-pot analysis was performed using PC-NPs upon incubation in complete HHPM (0–48 hours). The results revealed that PC-NPs immediately after incubation had a higher surface charge (approximately −21.4 mV; Fig. S6D, ESI†) compared to the bare PC-NPs (*i.e.*, dispersed in Milli-Q® water at pH of 8.5, Z-pot: −36.0 mV; see Fig. 3B). Such an increased surface charge remained stable over time, possibly indicating the presence of a bio-macromolecular corona around the PC-NPs.[70]

To disclose the possible impact of PC-NPs on the human liver, second-generation UHHs were acutely treated for 24 or 48 hours. Upon 24-hour exposure, the PC-NP dispersions showed no cytotoxic effect at any tested concentrations (20–100 μg mL^{-1}) (Fig. 5A). In fact, we found neither statistically significant alterations of cell viability compared to the control conditions nor a release of the cytosolic lactate dehydrogenase (LDH), which indicates the absence of cell membrane damage. Accordingly, cells treated with up to the highest concentration (100 μg mL^{-1}) appeared morphologically similar to the control cells (Fig. 5B). When the treatment lasted 48 hours, only the highest concentration of PC-NPs (100 μg mL^{-1}) determined a dramatic decrease of the cell viability to 8% with respect to the control ($p < 0.0001$), along with a significantly increased LDH release ($p = 0.0010$; Fig. 5C). Compared to the positive control, the LDH release induced by 100 μg mL^{-1} PC-NPs was equal to about 68% of the release obtained with 0.03% Triton X-100. Under the same conditions, treated cells showed dramatic morphological changes and reduced dimensions compared to the control cells (Fig. 5D). Recent studies employing the human hepatocarcinoma cell line HepG2 and acute 24-hour treatments investigated the toxicological impact of commercial PS-NPs (size: 50 nm, 10–100 μg mL^{-1}) with different surface chemistries (pristine and amino- or carboxy-modified NPs).[31] It was found that, independent from the NP functionalization, the cell viability was dose-dependently reduced, while the cell morphology was altered upon treatment of 100 μg mL^{-1} NPs. Similarly, Banerjee *et al.* showed that 100 μg mL^{-1} commercial aminated PS-NPs of various sizes (*i.e.*, 50–1000 nm) inhibited the HepG2 cell viability after 24 hours of treatment or earlier with the greater toxicity exhibited by 50 nm NPs, whereas for carboxylated PS-NPs only the smaller ones were toxic under the same conditions.[33] It has also been reported that 48 hours of

exposure with 25 μg mL^{-1} PS-NPs (30 nm), although it did not induce any significant cell viability variation in HepG2 cells, in line with our data, it determined a significant increase in binucleated cell rates, possibly indicative of impaired cytokinesis.[30] Hence, using a similar NP concentration range, it seems that PC- and PS-NPs exert comparable cytotoxicity in different human liver cell models. Taken together, these *in vitro* data suggest a moderate impact of nano-sized plastics on human cells upon treatment with concentrations higher than the ones predicted to be environmentally relevant (*e.g.*, from 1 pg L^{-1} to 15 μg L^{-1} for NPs at sizes of about 50 nm).[71] Considering polydisperse micro-sized plastic particles from different source materials, 24 hours of treatment with PP and PET particles (1–50 mg mL^{-1} and 1–100 mg mL^{-1}, respectively) did not impact the cell viability of both HepG2 and HepaRG cells, whereas PVC (100 mg mL^{-1}) and PE particles (50–100 mg mL^{-1}) were toxic to HepaRG and HepG2 cells, respectively,[32] indicating the differential toxicity of these micro-sized plastic types. Anyhow, none of these studies provided information on liver functionality and metabolism as the abovementioned cell models are unsuitable for such kinds of investigations.[35,36]

For a possible *in vivo* acute and chronic environmental exposure of the liver, where the NPs accumulate to the tissue, only concentrations lower than 40 μg mL^{-1} were selected for studying the interactions of PC-NPs with UHHs and some related specific metabolic functions. Using this range of concentrations, which is much lower than the toxic conditions shown above (*i.e.*, 100 μg mL^{-1}), we attempted to exclude unspecific metabolic alterations derived from a global cell impairment and, hence, to investigate the specific effects of PC-NPs on UHH functionality. Second-generation UHHs show transcriptional and functional features similar to PHHs, along with comparable toxicity profiles;[35,38,39,72] hence, the cytochrome P450 (CYP) system and albumin were chosen as hepatocyte-specific markers for assessing PC-NP hepatotoxicity. The CYP system includes several heme enzymes with a similar overall structure and shape, catalysing monooxygenations in the biosynthesis of endogenous compounds and the phase-I metabolism of xenobiotics/drugs.[73,74] Hence, the cytochrome P450 damage is directly linked to unexpected side effects during drug metabolism, for instance. In this study, four of the most abundant hepatic CYPs[75] were selected as representative targets (*i.e.*, CYP3A4, CYP2C9, CYP1A2, and CYP2B6) and their relative expression was monitored upon exposure of UHHs to PC-NPs. After 24 hours of treatment, the CYP3A4 gene expression was dose-dependently down-regulated, reaching a level equal to 0.11-fold with respect to the control ($p < 0.0001$) upon exposure to 40 μg mL^{-1} PC-NPs (Fig. 6A). Analogously, 40 μg mL^{-1} PC-NPs caused the significant down-regulation of the CYP2C9 gene expression, which was 0.42-fold lower than the control ($p < 0.0005$), while for lower concentrations no significant effects were observed. The highest concentration was also effective for the CYP1A2 gene expression but determined a significant 2.34-fold up-regulation of this CYP ($p < 0.0500$). Conversely, the gene expression of CYP2B6 was not affected by any tested concentration. When the exposure time was longer (48

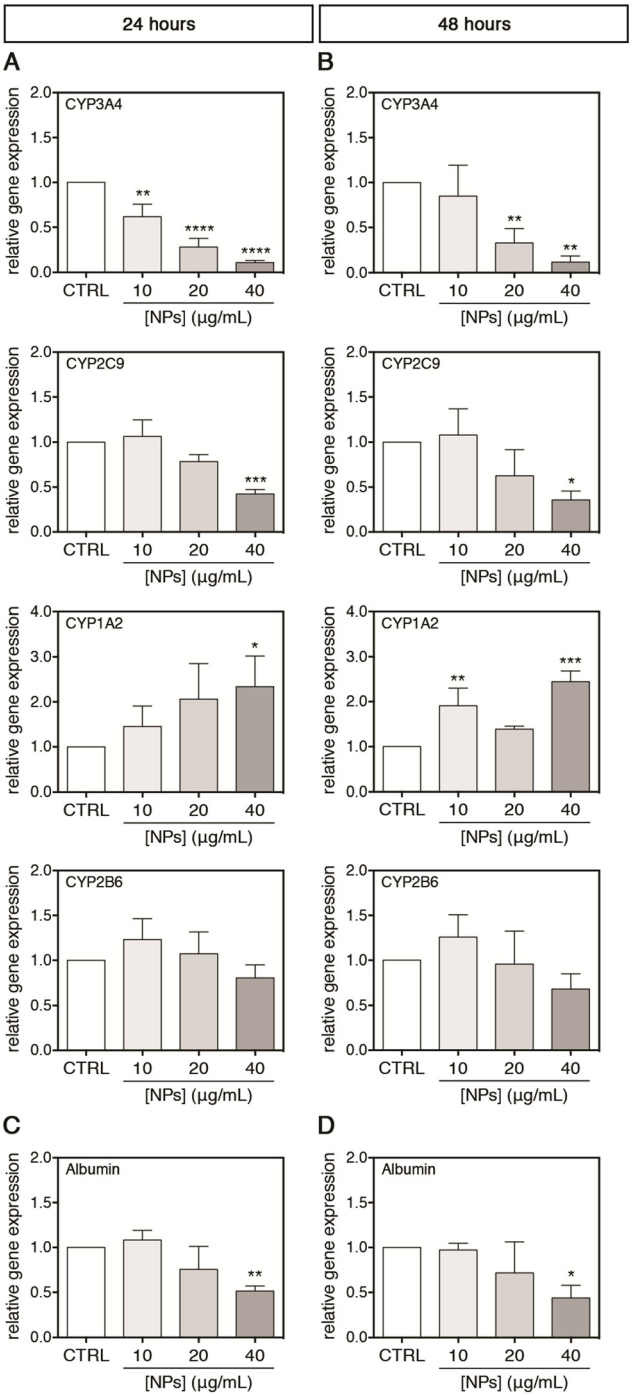

Fig. 6 PC-NP effects on the gene expression of the cytochrome P450 system and albumin. (A–D) Relative gene expression of four CYPs (CYP3A4, CYP2C9, CYP1A2 and CYP2B6) and albumin in cells treated with PC-NPs or untreated (indicated as CTRL) for 24 (A and C) and 48 hours (B and D). Results are reported as means ± SD of three independent experiments. The symbols *, **, *** and **** refer to $p < 0.0500$, $p < 0.0100$, $p < 0.0005$ and $p < 0.0001$, respectively, calculated *versus* CTRL for each treatment time (ordinary one-way ANOVA).

hours), the impact of 40 μg mL^{-1} PC-NPs on CYP3A4 and CYP2C9 did not change significantly compared to the 24 hours, having transcript levels equal to 0.11-fold (p = 0.0010) and 0.36-fold (p = 0.0100) lower than the control, respectively (Fig. 6B). This is also the case for the CYP1A2 transcription, which remained 2.45-fold up-regulated ($p < 0.0005$) upon treatment with 40 μg mL^{-1}; however, this effect was appreciated also at a lower dose (10 μg mL^{-1}) with the gene expression 1.91-fold up-regulated compared to the basal level ($p < 0.0050$). Conversely, the gene expression of CYP2B6 remained still unaltered at this longer time of incubation.

Afterward, the albumin production by UHHs was investigated upon treatment with PC-NPs (0–40 μg mL^{-1}) for 0–48 hours. Albumin is mainly synthesized *in vivo* by hepatocytes and is the most abundant plasmatic protein involved in maintaining blood colloid pressure and the binding and transport of endogenous molecules, ions, xenobiotics, and drugs.[76,77] This vast number of functions, along with the role as a negative acute-phase protein,[78] depicts the importance of albumin as a hepatic marker for the evaluation of hazard of potential toxicants. As shown in Fig. 6C and D, the treatment with 40 μg mL^{-1} PC-NPs resulted in the down-regulation of the albumin gene expression by 0.51-fold ($p < 0.0100$) and 0.44-fold ($p < 0.0500$) compared to the control after 24 and 48 hours of treatment, respectively.

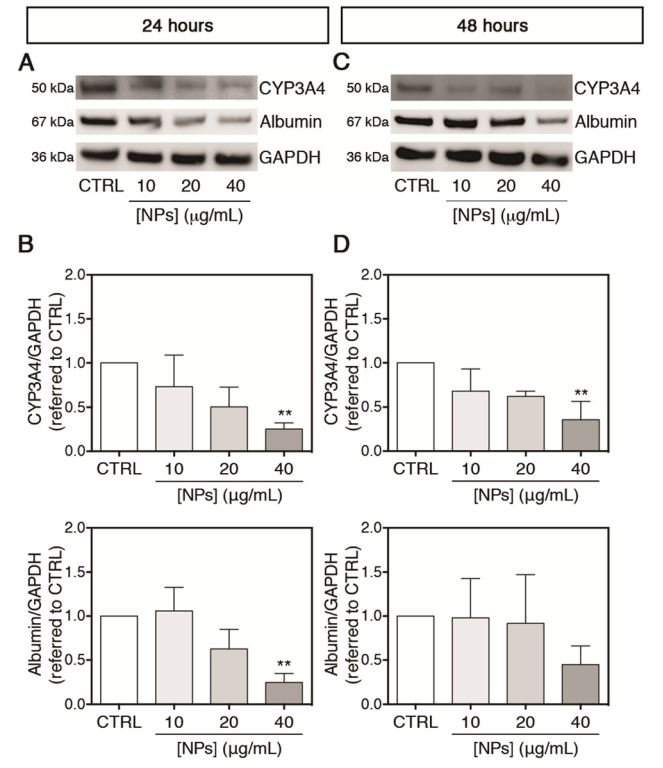

Fig. 7 PC-NP effects on translated protein amounts of CYP3A4 and albumin. (A and C) Representative western blots of total protein samples derived from cells treated with PC-NPs or un-treated for 24 (A) and 48 hours (C). (B and D) Densitometric analysis of three blots corresponding to independent experiments (means ± SD) for CYP3A4 (upper panel) and albumin (lower panel) levels upon 24 (B) and 48 hours of exposure (D). GAPDH was used as an internal control. Results are reported as n-fold increase over the control (indicated as CTRL). The symbol ** refers to $p < 0.0100$, calculated *versus* CTRL (ordinary one-way ANOVA).

After evaluating the effect of PC-NPs on the gene expression of some CYPs, the translated protein amounts of CYP3A4 (selected as representative among the tested CYPs) and albumin were also measured. As shown in Fig. 7A and B, accordingly to the gene expression up-regulation, the CYP3A4 protein level was significantly reduced to 0.25-fold with respect to the control ($p < 0.0100$) after exposure to 40 μg mL^{-1} PC-NPs for 24 hours, while at lower concentrations no statistically significant differences were observed. Under the same experimental conditions, similarly to the CYP3A4 gene expression, the cytoplasmic protein level of albumin was significantly decreased to 0.25-fold with respect to the control ($p < 0.0050$). After 48 hours, the CYP3A4 level was reduced to 0.36-fold compared to the control at 40 μg mL^{-1} ($p < 0.0050$), while no significant further decrease was evidenced for albumin (Fig. 7C and D). Since CYP3A4 is the most abundant CYP in the human liver and is involved in the metabolism of the majority of marketed drugs,[73,75] a down-regulated gene expression, corresponding also to a reduced amount of the translated protein, could determine undesired drug–drug interactions or impaired xenobiotic/drug detoxification.[79] Although not measured here, it is reasonable that a similar phenomenon of reduced protein translation can occur for CYP2C9 and CYP1A2, which were analogously found to be misregulated at the transcript level upon treatment of UHHs with PC-NPs. In support of that, the capability of CYP2C9 to metabolize the substrate MFC at the end of the PC-NP treatments was measured. We found that 40 μg mL^{-1} PC-NPs caused a significant inhibition of the CYP2C9 metabolic activity measuring approximately 54.1% and 72.9% of the basal level after 24 and 48 hours, respectively ($p < 0.0500$; Fig. S7A and B, ESI†). These data indicate that besides the alteration of the gene expression, its activity is also altered. In the literature, few data show the effects of NPs (from different commercial source materials) on the cytochrome P450 system, and, to the best of our knowledge, PHHs have not been used in any study. Fröhlich *et al.* reported that small (20–60 nm) carboxyl PS-NPs inhibited the metabolic activity of CYP3A4, CYP2D6, and CYP2C9 (less for CYP1A2) expressed individually in cell free based systems, the BACULOSOMES®, and inhibited the CYP3A4 and CYP2C9 activity in normal human liver microsomes.[80] It has been also shown that PS-NPs (approx. 75 nm) altered the gene expression of DpCYP370B, CYP4C33, CYP4C34, and CYP4AN1 in freshwater microcrustaceans (*Daphnia pulex*) after 21 days of dietary exposure.[81]

As far as albumin is concerned, severe PC-NP poisoning could induce hypoalbuminemia (*i.e.*, pathologically low levels of albumin in the blood), which, for instance, may impair pharmacokinetics of bound drugs and, in extreme

circumstances, may lead to abnormal accumulation of fluids into extravascular spaces.[76,82]

As discussed above, the laser ablation process produces a PC-NP dispersion composed not only of NPs but also of other photo-degradation by-products as may occur in the environmentally exposed plastic litter. Therefore, we investigated whether the soluble molecular matter, which includes the photo-degradation by-products, or the nano-particulate matter may have a role in determining the alteration of the metabolic functions of UHHs. To this aim, the dispersant deprived of PC-NPs and the isolated PC-NPs (for technical details, see the Materials and methods section) were tested separately on the cells using the same experimental design. The highest non-cytotoxic concentration selected in the previous experiments (*i.e.*, 40 μg mL^{-1}) was here applied for the treatment with isolated PC-NPs (which are retained by ultra-filtration), whereas the dispersant (which is the corresponding ultra-filtrate including the molecular matter) was supplemented to the complete HHPM by adding the same volume present in a 40 μg mL^{-1} conventional not-isolated PC-NP sample in order to obtain the same dilution factor. As shown in Fig. S8A and C,† after 24 hours of treatment, both the samples (isolated PC-NPs and dispersant) down-regulated the CYP3A4 gene expression, and this effect became more evident after 48 hours of treatment, indicating a detrimental impact induced by both the samples even though the observed effect was less pronounced than the conventional PC-NPs (see Fig. 6A and B). Notably, both the samples (isolated PC-NPs and dispersant) did not affect the albumin gene expression after 24 hours of treatment (Fig. S8B, ESI†), in contrast to the conventional PC-NPs (see Fig. 6C), whereas they down-regulated albumin only after 48 hours (Fig. S8D, ESI†). Taken together, these data suggest that the hepatotoxicity induced by PC-NPs to UHHs (*i.e.*, the altered gene expression of CYP3A4 and albumin) is likely mediated by both the components of PC-NPs, such as the nano-forms (*i.e.*, the fragments of NPs) and the soluble fraction of photo-degradation by-products. In fact, studies on the BPA leachate, which is identified in our work as a component of the photo-degradation by-products formed during the NP fabrication method, show that it inhibits the metabolic activity of some human CYPs, especially CYP2C8 and CYP2C19, expressed in microsomes,[37] and affects AhR, GR, and PXR signalling pathways, modulating the gene expression of downstream CYPs in human hepatocytes.[22] Additionally, BPA has been found to interact with CYP1A2, CYP2A2, CYP2B2, CYP2C11, CYP2D1, CYP2E1, and CYP3A2 in rat liver microsomes.[83] Keeping in mind these data, it is completely plausible to find hepatocyte-specific function alterations exerted by the dispersant in addition to the impact of isolated PC-NPs, as we described above.

Hence, the approach used herein to separate and assess the components of PC-NPs represents a novel aspect of our work since the current data on plastic particle-induced hepatotoxicity have been largely produced using commercially available products, potentially underestimating the real impact of the photo-degradation process, which produces other toxicants apart from the particles. Consistent with our findings, Wang *et al.* found that photo-degradation of PS-MPs enhanced the hepatotoxicity of pristine MPs in juvenile groupers (*Epinephelus moara*), and such an impact was mainly due to increased hepatic bioaccumulation of the photo-degraded PS-MPs and of other endogenous pollutants leached from the polymer during the photo-degradation process.[20] It should be mentioned that regardless of the few and sparse information on environmental exposure doses,[71] the established concentration range in the order of μg mL^{-1} was to simulate a worst case scenario related to the accumulation of NPs, which may be the conditions likely occurring in an excretion organ such as the liver.[84] Nonetheless, further studies are needed in order to precisely define the effects of the chronic exposure on UHHs using lower concentrations, closer to the environmental values, and repeated doses.

Conclusions

The production of a realistic model of PC photo-degradation products was achieved through a top-down laser ablation technique. Chemical analysis demonstrated that the composition of the ablation product was similar to the one coming from the photo-degraded PC plastic exposed to the environment. Hepatotoxicity studies revealed that no effects were induced by the PC-NP dispersion (exposure up to 40 μg mL^{-1} for up to 48 hours) in terms of cell viability impairment or cell membrane damage. However, the gene expression of 3 out of 4 cytochromes P450 (CYP3A4, CYP2C9, and CYP1A2) was misregulated, and albumin was also down-regulated. This detrimental impact was further evidenced by a reduced protein level for CYP3A4 and albumin. Interestingly, these alterations were observed at concentrations that are sub-lethal for UHHs and upon acute exposure, thus evidencing that potentially chronic exposure to PC-NPs (as likely may occur in humans over the entire lifetime) may cause severe effects. The harmful effects evidenced in this study are mediated by both the nano-particulate matter and the photo-degradation molecular by-products, but they are better appreciated and higher in the complete PC-NP dispersion. UHHs are, thus, presented herein as a suitable *in vitro* model for testing NPs and their toxicity to the human liver. Although the induced hazard is strictly related to an altered expression of cytochromes P450 and albumin, we cannot exclude that other liver markers can be affected and will be the object of further future studies. In conclusion, the impact of PC-NPs on humans could be related to the alteration of specific hepatic functionalities such as the body's drug/toxicant detoxification, drug–drug interactions, and/or drug pharmacokinetics. To further investigate these functions, we underline the importance of mature technologies for

the production of environmentally pertinent NP samples, as well as the use of suitable *in vitro* human liver models.

Author contributions

Valentina Tolardo: investigation, methodology, visualization, writing – original draft. Alessio Romaldini: investigation, methodology, visualization, writing – original draft. Francesco Fumagalli: investigation, writing – review & editing. Andrea Armirotti: investigation, writing – review & editing. Marina Veronesi: investigation, writing – review & editing. Davide Magri: writing – review & editing. Stefania Sabella: conceptualization, validation, methodology, visualization, writing – review & editing, supervision. Athanassia Athanassiou: funding acquisition, writing – review & editing. Despina Fragouli: conceptualization, validation, methodology, visualization, writing – original draft, supervision.

Conflicts of interest

There are no conflicts to declare.

Acknowledgements

This research did not receive any specific grant from funding agencies in the public, commercial, or not-for-profit sectors. The authors thank Lara Marini, Riccardo Carzino, and Federico Catalano from Istituto Italiano di Tecnologia, and Giacomo Ceccone, Sabrina Gioria and Douglas Gilliland from EU-JRC Ispra, Unit F.2 Nanobiotechnology Lab, for the valuable discussions and technical help. The authors acknowledge the Sustainability Initiative of Istituto Italiano di Tecnologia.

References

1 R. A. Sheldon and M. Norton, Green chemistry and the plastic pollution challenge: towards a circular economy, *Green Chem.*, 2020, **22**, 6310–6322.
2 L. E. Haram, J. T. Carlton, G. M. Ruiz and N. A. Maximenko, A Plasticene Lexicon, *Mar. Pollut. Bull.*, 2020, **150**, 110714.
3 UNEP (United Nations Environment Programme), *From pollution to solution: a global assessment of marine litter and plastic pollution*, 2021, vol. 237.
4 W. W. Y. Lau, Y. Shiran, R. M. Bailey, E. Cook, M. R. Stuchtey, J. Koskella, C. A. Velis, L. Godfrey, J. Boucher, M. B. Murphy, R. C. Thompson, E. Jankowska, A. Castillo Castillo, T. D. Pilditch, B. Dixon, L. Koerselman, E. Kosior, E. Favoino, J. Gutberlet, S. Baulch, M. E. Atreya, D. Fischer, K. K. He, M. M. Petit, U. R. Sumaila, E. Neil, M. V. Bernhofen, K. Lawrence and J. E. Palardy, Evaluating scenarios toward zero plastic pollution, *Science*, 2020, **369**, 1455–1461.
5 C. Wabnitz and W. J. Nichols, Editorial: Plastic Pollution: An Ocean Emergency, *Marine Turtle Newsletter*, 2010, vol. 129, pp. 1–4.
6 A. L. Lusher, V. Tirelli, I. O'Connor and R. Officer, Microplastics in Arctic polar waters: The first reported values of particles in surface and sub-surface samples, *Sci. Rep.*, 2015, **5**, 1–9.
7 M. Bergmann, F. Collard, J. Fabres, G. W. Gabrielsen, J. F. Provencher, C. M. Rochman, E. van Sebille and M. B. Tekman, Plastic pollution in the Arctic, *Nat. Rev. Earth Environ.*, 2022, **3**, 323–337.
8 M. Kosuth, S. A. Mason and E. V. Wattenberg, Anthropogenic contamination of tap water, beer, and sea salt, *PLoS One*, 2018, **13**, e0194970.
9 J. Zhang, L. Wang, L. Trasande and K. Kannan, Occurrence of Polyethylene Terephthalate and Polycarbonate Microplastics in Infant and Adult Feces, *Environ. Sci. Technol. Lett.*, 2021, **8**, 989–994.
10 J. Zhang, L. Wang and K. Kannan, Polyethylene Terephthalate and Polycarbonate Microplastics in Pet Food and Feces from the United States, *Environ. Sci. Technol.*, 2019, **53**, 12035–12042.
11 H. A. Leslie, M. J. M. van Velzen, S. H. Brandsma, D. Vethaak, J. J. Garcia-Vallejo and M. H. Lamoree, Discovery and quantification of plastic particle pollution in human blood, *Environ. Int.*, 2022, 107199.
12 Y. Zhang, A. Diehl, A. Lewandowski, K. Gopalakrishnan and T. Baker, Removal efficiency of micro- and nanoplastics (180 nm–125 μm) during drinking water treatment, *Sci. Total Environ.*, 2020, **720**, 137383.
13 C. Schwaferts, R. Niessner, M. Elsner and N. P. Ivleva, Methods for the analysis of submicrometer- and nanoplastic particles in the environment, *TrAC, Trends Anal. Chem.*, 2019, **112**, 52–65.
14 J. N. Möller, M. G. J. Löder and C. Laforsch, Finding Microplastics in Soils: A Review of Analytical Methods, *Environ. Sci. Technol.*, 2020, **54**, 2078–2090.
15 O. Pikuda, E. G. Xu, D. Berk and N. Tufenkji, Toxicity Assessments of Micro- and Nanoplastics Can Be Confounded by Preservatives in Commercial Formulations, *Environ. Sci. Technol. Lett.*, 2019, **6**, 21–25.
16 M. Almeida, M. A. Martins, A. M. V. Soares, A. Cuesta and M. Oliveira, Polystyrene nanoplastics alter the cytotoxicity of human pharmaceuticals on marine fish cell lines, *Environ. Toxicol. Pharmacol.*, 2019, **69**, 57–65.
17 T. Ö. Sökmen, E. Sulukan, M. Türkoğlu, A. Baran, M. Özkaraca and S. B. Ceyhun, Polystyrene nanoplastics (20 nm) are able to bioaccumulate and cause oxidative DNA damages in the brain tissue of zebrafish embryo (Danio rerio), *Neurotoxicology*, 2020, **77**, 51–59.
18 J. P. da Costa, P. S. M. Santos, A. C. Duarte and T. Rocha-Santos, (Nano)plastics in the environment – Sources, fates and effects, *Sci. Total Environ.*, 2016, **566–567**, 15–26.
19 A. L. Andrady, Microplastics in the marine environment, *Mar. Pollut. Bull.*, 2011, **62**, 1596–1605.
20 X. Wang, H. Zheng, J. Zhao, X. Luo, Z. Wang and B. Xing, Photodegradation Elevated the Toxicity of Polystyrene Microplastics to Grouper (Epinephelus moara) through Disrupting Hepatic Lipid Homeostasis, *Environ. Sci. Technol.*, 2020, **54**, 6202–6212.

21 Y. Shi, P. Liu, X. Wu, H. Shi, H. Huang, H. Wang and S. Gao, Insight into chain scission and release profiles from photodegradation of polycarbonate microplastics, *Water Res.*, 2021, **195**, 116980.
22 R. Vrzal, O. Zenata, A. Doricakova and Z. Dvorak, Environmental pollutants parathion, paraquat and bisphenol A show distinct effects towards nuclear receptors-mediated induction of xenobiotics-metabolizing cyt ochromes P450 in human hepatocytes, *Toxicol. Lett.*, 2015, **238**, 43–53.
23 B. Toussaint, B. Raffael, A. Angers-Loustau, D. Gilliland, V. Kestens, M. Petrillo, I. M. Rio-Echevarria and G. Van den Eede, Review of micro- and nanoplastic contamination in the food chain, *Food Addit. Contam., Part A*, 2019, **36**, 639–673.
24 EFSA CONTAM Panel (EFSA Panel on Contaminants in the Food Chain), Statement on the presence of microplastics and nanoplastics in food, with particular focus on seafood, *EFSA J.*, 2016, **14**(6), 4501.
25 M. Revel, A. Châtel and C. Mouneyrac, Micro(nano)plastics: A threat to human health?, *Curr. Opin. Environ. Sci. Health*, 2018, **1**, 17–23.
26 Y. Deng, Y. Zhang, B. Lemos and H. Ren, Tissue accumulation of microplastics in mice and biomarker responses suggest widespread health risks of exposure, *Sci. Rep.*, 2017, **7**, 46687.
27 P. Jani, G. W. Halbert, J. Langridge and A. T. Florence, Nanoparticle Uptake by the Rat Gastrointestinal Mucosa: Quantitation and Particle Size Dependency, *J. Pharm. Pharmacol.*, 1990, **42**, 821–826.
28 Y. Chae, D. Kim, S. W. Kim and Y.-J. An, Trophic transfer and individual impact of nano-sized polystyrene in a four-species freshwater food chain, *Sci. Rep.*, 2018, **8**, 284.
29 I. Brandts, M. Teles, A. Tvarijonaviciute, M. L. Pereira, M. A. Martins, L. Tort and M. Oliveira, Effects of polymethylmethacrylate nanoplastics on Dicentrarchus labrax, *Genomics*, 2018, **110**, 435–441.
30 L. Xia, W. Gu, M. Zhang, Y.-N. Chang, K. Chen, X. Bai, L. Yu, J. Li, S. Li and G. Xing, Endocytosed nanoparticles hold endosomes and stimulate binucleated cells formation, *Part. Fibre Toxicol.*, 2016, **13**, 63.
31 Y. He, J. Li, J. Chen, X. Miao, G. Li, Q. He, H. Xu, H. Li and Y. Wei, Cytotoxic effects of polystyrene nanoplastics with different surface functionalization on human HepG2 cells, *Sci. Total Environ.*, 2020, **723**, 138180.
32 V. Stock, C. Laurisch, J. Franke, M. H. Dönmez, L. Voss, L. Böhmert, A. Braeuning and H. Sieg, Uptake and cellular effects of PE, PP, PET and PVC microplastic particles, *Toxicol. In Vitro*, 2021, **70**, 105021.
33 A. Banerjee, L. O. Billey, A. M. McGarvey and W. L. Shelver, Effects of polystyrene micro/nanoplastics on liver cells based on particle size, surface functionalization, concentration and exposure period, *Sci. Total Environ.*, 2022, **836**, 155621.
34 V. Tolardo, D. Magrì, F. Fumagalli, D. Cassano, A. Athanassiou, D. Fragouli and S. Gioria, In Vitro High-Throughput Toxicological Assessment of Nanoplastics, *Nanomaterials*, 2022, **12**, 1947.
35 L. Tolosa, M. J. Gómez-Lechón, S. López, C. Guzmán, J. V. Castell, M. T. Donato and R. Jover, Human upcyte hepatocytes: Characterization of the hepatic phenotype and evaluation for acute and long-term hepatotoxicity routine testing, *Toxicol. Sci.*, 2016, **152**, 214–229.
36 W. M. A. Westerink and W. G. E. J. Schoonen, Cytochrome P450 enzyme levels in HepG2 cells and cryopreserved primary human hepatocytes and their induction in HepG2 cells, *Toxicol. In Vitro*, 2007, **21**, 1581–1591.
37 T. Niwa, M. Tsutsui, K. Kishimoto, Y. Yabusaki, F. Ishibashi and M. Katagiri, Inhibition of Drug-Metabolizing Enzyme Activity in Human Hepatic Cytochrome P450s by Bisphenol A, *Biol. Pharm. Bull.*, 2000, **23**, 498–501.
38 G. Levy, D. Bomze, S. Heinz, S. D. Ramachandran, A. Noerenberg, M. Cohen, O. Shibolet, E. Sklan, J. Braspenning and Y. Nahmias, Long-term culture and expansion of primary human hepatocytes, *Nat. Biotechnol.*, 2015, **33**, 1264–1271.
39 M. Schaefer, G. Schanzle, D. Bischoff and R. D. Sussmuth, Upcyte Human Hepatocytes: a Potent In Vitro Tool for the Prediction of Hepatic Clearance of Metabolically Stable Compounds, *Drug Metab. Dispos.*, 2016, **44**, 435–444.
40 I. Elaboudi, S. Lazare, C. Belin, J. L. Bruneel and L. Servant, Organic nanoparticles suspensions preparation by underwater excimer laser ablation of polycarbonate, *Appl. Surf. Sci.*, 2007, **253**, 7835–7839.
41 I. Elaboudi, S. Lazare, C. Belin, D. Talaga and C. Labrugère, From polymer films to organic nanoparticles suspensions by means of excimer laser ablation in water, *Appl. Phys. A: Mater. Sci. Process.*, 2008, **93**, 827–831.
42 D. Magrì, P. Sánchez-Moreno, G. Caputo, F. Gatto, M. Veronesi, G. Bardi, T. Catelani, D. Guarnieri, A. Athanassiou, P. P. Pompa and D. Fragouli, Laser Ablation as a Versatile Tool To Mimic Polyethylene Terephthalate Nanoplastic Pollutants: Characterization and Toxicology Assessment, *ACS Nano*, 2018, **12**, 7690–7700.
43 FDA, Guidance for Industry Pyrogen and Endotoxins Testing: Questions and Answers, *Guidance Document*, 2012, vol. 1, pp. 1–10.
44 A. Romaldini, R. Spanò, F. Catalano, F. Villa, A. Poggi and S. Sabella, Sub-Lethal Concentrations of Graphene Oxide Trigger Acute-Phase Response and Impairment of Phase-I Xenobiotic Metabolism in Upcyte® Hepatocytes, *Front. Bioeng. Biotechnol.*, 2022, **10**, 867728.
45 D. Magrì, M. Veronesi, P. Sánchez-Moreno, V. Tolardo, T. Bandiera, P. P. Pompa, A. Athanassiou and D. Fragouli, PET nanoplastics interactions with water contaminants and their impact on human cells, *Environ. Pollut.*, 2020, **271**, 116262.
46 P. Lemoine and W. Blau, Photoablation of polymers, *Appl. Surf. Sci.*, 1992, **54**, 240–243.
47 P. K. Goyal, V. Kumar, R. Gupta, S. Mahendia, Anita and S. Kumar, Modification of polycarbonate surface by Ar + ion implantation for various opto-electronic applications, *Vacuum*, 2012, **86**, 1087–1091.

48 V. Resta, G. Quarta, M. Lomascolo, L. Maruccio and L. Calcagnile, Raman and Photoluminescence spectroscopy of polycarbonate matrices irradiated with different energy 28Si + ions, *Vacuum*, 2015, **116**, 82–89.
49 S. Bahniwal, A. Sharma, S. Aggarwal, S. K. Deshpande, S. K. Sharma and K. G. M. Nair, Changes in structural and optical properties of polycarbonate induced by Ag+ Ion implantation, *J. Macromol. Sci., Part B: Phys.*, 2010, **49**, 259–268.
50 P. Sánchez-Moreno, J. L. Ortega-Vinuesa, A. Martín-Rodríguez, H. Boulaiz, J. A. Marchal-Corrales and J. M. Peula-García, Characterization of different functionalized lipidic nanocapsules as potential drug carriers, *Int. J. Mol. Sci.*, 2012, **13**, 2405–2424.
51 T. R. Gengenbach, G. H. Major, M. R. Linford and C. D. Easton, Practical guides for x-ray photoelectron spectroscopy (XPS): Interpreting the carbon 1s spectrum, *J. Vac. Sci. Technol., A*, 2021, **39**, 013204.
52 Y. Jia, H. Asahara, Y. I. Hsu, T. A. Asoh and H. Uyama, Surface modification of polycarbonate using the light-activated chlorine dioxide radical, *Appl. Surf. Sci.*, 2020, **530**, 147202.
53 L. Jahnke, A. White and P. Sampath-Wiley, in *The Alga Dunaliella*, Science Publishers, 2009, pp. 231–272.
54 G. J. Pratt and M. J. A. Smith, Ultraviolet degradation and stabilization in poly(dian carbonate): Dielectric measurements, *Polym. Degrad. Stab.*, 1989, **25**, 267–276.
55 G. J. Pratt and M. J. A. Smith, Ultraviolet degradation and stabilization in poly(dian carbonate): Dielectric measurements - II, *Polym. Degrad. Stab.*, 1997, **56**, 179–183.
56 B. W. Muir, S. L. Mc Arthur, H. Thissen, G. P. Simon, H. J. Griesser and D. G. Castner, Effects of oxygen plasma treatment on the surface of bisphenol A polycarbonate: A study using SIMS, principal component analysis, ellipsometry, XPS and AFM nanoindentation, *Surf. Interface Anal.*, 2006, **38**, 1186–1197.
57 F. Blancho, M. Davranche, F. Fumagalli, G. Ceccone and J. Gigault, A reliable procedure to obtain environmentally relevant nanoplastic proxies, *Environ. Sci.: Nano*, 2021, **8**, 3211–3219.
58 A. Rivaton, D. Sallet and J. Lemaire, The photochemistry of bisphenol-A polycarbonate reconsidered, *Polym. Photochem.*, 1983, **3**, 463–481.
59 D. T. Clark and H. S. Munro, Surface and bulk aspects of the natural and artificial photo-ageing of Bisphenol A polycarbonate as revealed by ESCA and difference UV spectroscopy, *Polym. Degrad. Stab.*, 1984, **8**, 195–211.
60 D. T. Clark and H. S. Munro, Surface aspects of the photo-degradation of bisphenol A polycarbonate, in oxygen and air as a function of relative humidity, as revealed by ESCA, *Polym. Degrad. Stab.*, 1983, **5**, 227–236.
61 D. T. Clark and H. S. Munro, Surface aspects of the photodegradation of bisphenol a polycarbonate in oxygen and nitrogen atmospheres as revealed by ESCA, *Polym. Degrad. Stab.*, 1982, **4**, 441–457.
62 M. Diepens and P. Gijsman, Photodegradation of bisphenol A polycarbonate, *Polym. Degrad. Stab.*, 2007, **92**, 397–406.
63 A. Rivaton, D. Sallet and J. Lemaire, The photo-chemistry of bisphenol-A polycarbonate reconsidered: Part 3-Influence of water on polycarbonate photo-chemistry, *Polym. Degrad. Stab.*, 1986, **14**, 23–40.
64 M. Diepens and P. Gijsman, Outdoor and accelerated weathering studies of bisphenol A polycarbonate, *Polym. Degrad. Stab.*, 2011, **96**, 649–652.
65 A. O. Kondrakov, A. N. Ignatev, F. H. Frimmel, S. Bräse, H. Horn and A. I. Revelsky, Formation of genotoxic quinones during bisphenol A degradation by TiO2 photocatalysis and UV photolysis: A comparative study, *Appl. Catal., B*, 2014, **160–161**, 106–114.
66 D. P. Subagio, M. Srinivasan, M. Lim and T. T. Lim, Photocatalytic degradation of bisphenol-A by nitrogen-doped TiO2 hollow sphere in a vis-LED photoreactor, *Appl. Catal., B*, 2010, **95**, 414–422.
67 T. Olmez-Hanci, I. Arslan-Alaton and B. Genc, Bisphenol A treatment by the hot persulfate process: Oxidation products and acute toxicity, *J. Hazard. Mater.*, 2013, **263**, 283–290.
68 H. P. H. Arp, D. Kühnel, C. Rummel, M. MacLeod, A. Potthoff, S. Reichelt, E. Rojo-Nieto, M. Schmitt-Jansen, J. Sonnenberg, E. Toorman and A. Jahnke, Weathering Plastics as a Planetary Boundary Threat: Exposure, Fate, and Hazards, *Environ. Sci. Technol.*, 2021, **55**, 7246–7255.
69 B. Gewert, M. Plassmann, O. Sandblom and M. Macleod, Identification of Chain Scission Products Released to Water by Plastic Exposed to Ultraviolet Light, *Environ. Sci. Technol. Lett.*, 2018, **5**, 272–276.
70 G. Maiorano, S. Sabella, B. Sorce, V. Brunetti, M. A. Malvindi, R. Cingolani and P. P. Pompa, Effects of Cell Culture Media on the Dynamic Formation of Protein –Nanoparticle Complexes and Influence on the Cellular Response, *ACS Nano*, 2010, **4**, 7481–7491.
71 R. Lehner, C. Weder, A. Petri-Fink and B. Rothen-Rutishauser, Emergence of Nanoplastic in the Environment and Possible Impact on Human Health, *Environ. Sci. Technol.*, 2019, **53**, 1748–1765.
72 L. Tolosa, N. Jiménez, M. Pelechá, J. V. Castell, M. J. Gómez-Lechón and M. T. Donato, Long-term and mechanistic evaluation of drug-induced liver injury in Upcyte human hepatocytes, *Arch. Toxicol.*, 2019, **93**, 519–532.
73 P. Anzenbacher and E. Anzenbacherová, Cytochromes P450 and metabolism of xenobiotics, *Cell. Mol. Life Sci.*, 2001, **58**, 737–747.
74 A. Kawashima and Y. Satta, Substrate-Dependent Evolution of Cytochrome P450: Rapid Turnover of the Detoxification-Type and Conservation of the Biosynthesis-Type, *PLoS One*, 2014, **9**, e100059.
75 B. Achour, J. Barber and A. Rostami-Hodjegan, Expression of Hepatic Drug-Metabolizing Cytochrome P450 Enzymes and Their Intercorrelations: A Meta-Analysis, *Drug Metab. Dispos.*, 2014, **42**, 1349–1356.
76 M. Chojkier, Inhibition of Albumin Synthesis in Chronic Diseases, *J. Clin. Gastroenterol.*, 2005, **39**, S143–S146.

77 A. M. Merlot, D. S. Kalinowski and D. R. Richardson, Unraveling the mysteries of serum albumin-more than just a serum protein, *Front. Physiol.*, 2014, **5**, 299.
78 C. Gabay and I. Kushner, Acute-Phase Proteins and Other Systemic Responses to Inflammation, *N. Engl. J. Med.*, 1999, **340**, 448–454.
79 O. Pelkonen, M. Turpeinen, J. Hakkola, P. Honkakoski, J. Hukkanen and H. Raunio, Inhibition and induction of human cytochrome P450 enzymes: current status, *Arch. Toxicol.*, 2008, **82**, 667–715.
80 E. Fröhlich, T. Kueznik, C. Samberger, E. Roblegg, C. Wrighton and T. R. Pieber, Size-dependent effects of nanoparticles on the activity of cytochrome P450 isoenzymes, *Toxicol. Appl. Pharmacol.*, 2010, **242**, 326–332.
81 D. Wu, Z. Liu, M. Cai, Y. Jiao, Y. Li, Q. Chen and Y. Zhao, Molecular characterisation of cytochrome P450 enzymes in waterflea (Daphnia pulex) and their expression regulation by polystyrene nanoplastics, *Aquat. Toxicol.*, 2019, **217**, 105350.
82 A. Gatta, A. Verardo and M. Bolognesi, Hypoalbuminemia, *Intern. Emerg. Med.*, 2012, **7**, 193–199.
83 N. Hanioka, H. Jinno, T. Tanaka-Kagawa, T. Nishimura and M. Ando, Interaction of bisphenol A with rat hepatic cytochrome P450 enzymes, *Chemosphere*, 2000, **41**, 973–978.
84 Y. Ding, R. Zhang, B. Li, Y. Du, J. Li, X. Tong, Y. Wu, X. Ji and Y. Zhang, Tissue distribution of polystyrene nanoplastics in mice and their entry, transport, and cytotoxicity to GES-1 cells, *Environ. Pollut.*, 2021, **280**, 116974.